Romanian Reports in Physics, Vol. 67, No. 4, P. 1251–1260, 2015

Dedicated to
International Year of Light 2015

HIGH-INTENSITY THz PULSES APPLICATION TO PROTEIN CONFORMATIONAL CHANGES

O. GRIGORE[1,2], O. CALBOREAN[3], G. COJOCARU[1,2], R. UNGUREANU[1,2], M. MERNEA[3], M.P. DINCA[1,2], S. AVRAM[3], D.F. MIHAILESCU[3], T. DASCALU[1,*]

[1] National Institute for Laser Plasma and Radiation Physics, P.O. Box MG-36, 077125 Bucharest – Magurele, Romania,
E-mails: oana.grigore@inflpr.ro, gabriel.cojocaru@inflpr.ro, razvan.ungureanu@inflpr.ro, traian.dascalu@inflpr.ro
[2] University of Bucharest, Faculty of Physics, P.O. Box MG-11, 077125, Bucharest – Magurele, Romania, E-mail: mpdinca@gmail.com
[3] University of Bucharest, Faculty of Biology, 91–95 Splaiul Independentei, Sector 5, 050095, Bucharest, Romania, E-mail: dan.mihailescu@bio.unibuc.ro
*Corresponding author: traian.dascalu@inflr.ro

Received October 7, 2015

Abstract. A new method for conformational changes of enzymes under very intense and short electric field is proposed. The molecular dynamics of linoleate 9/13-lipoxygenase from *Pseudomonas aeruginosa* was simulated for frequencies ranging from 1 to 15 THz under electric field of 10^7 V/m with pulse length of 2 ps. Multiple intense THz field is generated by combining two-color plasma filamentation with a method for splitting and delaying short laser pulses. Large conformational changes of protein structure are predicted by using μJ THz pulse energy with 15 THz bandwidth.

Key words: THz generation, THz Spectroscopy, multiple THz pulses, two color filamentation, proteins, molecular modeling.

1. INTRODUCTION

Many of the present diseases are due to the misfolding of the proteins. For example, amyloid protein is responsible of more than 20 serious human diseases, like Alzheimer, Parkinson, etc. In 2009, Toschi *et al.* [1] investigated by molecular dynamic simulation the interaction of beta-amyloid (Abeta) peptides with externally applied electric fields (EF) of varying strengths. The results suggest that the EF favors the switch of Abeta-peptides from helical to beta-sheet conformation, and switching off the field does not restore the original conformation. Intense electric field applied for short period within the frequency range compatible with molecular spectra seems to be the next step in further investigation of proteins functionality.

The rotational and vibrational modes of many molecules, especially organic ones, are distributed across the THz band [2] and these modes can be observed as

absorption peaks in the THz spectra. The specific location and amplitude of these absorption peaks can be used to identify the molecules [3]. Better understanding of protein function and especially of enzymes requires the study of their conformational transitions. One way to obtain conformational changes without destroying its morphology is using intense electric fields at THz wavelength because the low energy of THz photons (meV) do not harm intrinsic structure of the proteins.

Lipoxygenases are a class of nonheme iron containing enzymes that are essential for eukaryotic cells metabolism, but are rarely expressed in bacteria. Linoleate 9/13-lipoxygenase from *Pseudomonas aeruginosa* bacteria is a 685 amino-acid enzyme whose main function is to alter the properties of host cell membranes by oxidation of their unsaturated phospholipids. Its complete 3D structure bound to a lipid substrate was recently discovered, and it was shown to present major differences from those of eukaryotic lipoxygenases [4]. Lipids oxidation by lipoxygenases results in the production of free radicals that have a damaging effect on proteins and DNA. In humans, severe diseases like diabetes, atherosclerosis or liver disease are characterized by high levels of lipid oxidation products [5]. The flexibility of lipoxygenases is a key feature for their function, as enzymes with increased rigidity due to an active site ligand are unable to bind the membranes [6].

THz sources are characterized by wavelengths of hundred times longer than infrared wavelengths and ten times shorter than those from radiofrequency range. Many common materials and living tissues are semi-transparent and have 'terahertz fingerprints', permitting them to be imaged, identified, and analyzed. Applications of THz radiation also include quality control of manufacturing processes [7], tomography [8] and security [9]. In particular, high intensity THz pulses are attractive for biomedical applications, such as medical imaging [10], DNA analyses [11] and validation of theoretical protein structural models [3]. All these investigations were done alongside developments of THz sources. The most intense and widely used THz sources are laser based sources, no matter if one can talk about applying photoconductive excitation on biased semiconductors [12], difference-frequency generation in electro-optic crystals, [13, 14] or laser plasma generation in different gaseous media [15].

Here we address the computer simulation of conformational changes of linoleate 9/13-lipoxygenase from *Pseudomonas aeruginosa* when exposed to a THz pulse with the maximum intensity (E_{max}) used in experiments, namely 10^7 V/m. In order to achieve our aim, we decomposed the pulse in frequencies ranging from 1 THz to 15 THz and simulated the molecular dynamics (MD) of the protein at each frequency in an electric field with the corresponding intensity as given by the formula:

$$E_\omega = E_{max} \cos(\omega t). \quad (1)$$

The dynamics at each frequency was simulated for 2 ps, the length of the very intense THz pulse described in experiments. To prepare the experimental proof of the numerical results we developed a multiple very intense THz pulses source that delivers trains of pulses with controllable delay from 1 ps to 100 ps and 2 ps pulse width.

The intense THz pulses generation method is based on two-color air filamentation using a device formed by a thin film beam splitter (TFBS) and a mirror. THz pulse energy obtained by this method exceeds the energy achieved by classical method of two-color plasma filament.

2. MOLECULAR MODELING UNDER INTENSE THz FIELD

2.1. MATERIALS AND METHODS

All the molecular modeling simulations were done using the CHARMM version 37b2 modeling software [16] with the CHARMM force field version 39b1 [17] on a Intel eon CPU E5-2670 at 2.60 GHz (dual octa-core) server with 64 GB 1600 MHz RAM and running Scientific Linux release 6.7 64bit operating system.

We used the known 3D structure of *Pseudomonas aeruginosa* linoleate 9/13-lipoygenase (PDB ID: 4G33) [4]. We removed all non-protein atoms, added the hydrogen atoms to the protein, minimized the structures (200 steps of Steepest Descent and 200 steps of Adopted Basis Newton-Raphson) and performed two 3 ns Langevin MD simulations at 298 K for equilibration: one using an EEF1 implicit solvation model [18] and one in vacuum. In both simulations, we used a 2 fs time step and fixed all bond lengths involving hydrogen atoms with the SHAKE algorithm [19].

After equilibration, we run 15 consecutive Langevin MD simulations at 298 K of 2 ps each applying a variable electric field with an intensity of 10^7 V/m oriented along the *x* axis (Fig. 2). We started with a 1 THz electric field frequency, and at the end of each 2 ps of simulation, we increased the frequency by 1 THz until we reached 15 THz in the last simulation. As control, we performed a 30 ps Langevin MD simulation in the absence of an electric field. The rotation and translation motions of the simulation system were prevented by reducing the step frequency for stopping it (NTRFRQ) to once every 20 fs. Two sets of calculations were performed, with implicit solvent and in vacuum.

Resulting trajectories were analyzed in order to identify the conformational changes occurring due to the applied electric field. The equilibrated structure can be compared to the conformations adopted during MD by calculating the

root-mean-square deviation (RMSD) of backbone atomic positions. RMSD is calculated based on the structures with superimposed backbones and it is given by the formula:

$$\text{RMSD} = \text{sqrt}\,[1/N\,(\Sigma_{i=1}{}^{N}\delta_i{}^{2})], \tag{2}$$

where δ is the distance between the N pairs of atoms [20]. RMSD time series for the electric field and control simulations relative to the equilibrated structures were calculated using VMD software [21].

2.2. SIMULATION RESULTS

RMSD values calculated for *Pseudomonas aeruginosa* linoleate 9/13-lipoxygenase during the control and electric field MD simulations in implicit solvent relative to the equilibrated structure are presented in Fig. 1a. Those resulting from the simulations in vacuum are presented in Fig. 1b. As can be seen, both in vacuum and in implicit solvent, the molecule in control simulations enters a stable state after ~3 ps. When the structure is exposed to the eternal applied electric field, in both cases, the RMSD presents a steady increase until the end of the simulations. In comparison to the control, RMSD presents a difference of ~1.5 Å in the simulations performed in implicit solvent and ~0.8 Å in the simulations performed in vacuum. In Fig. 2 we present the structure of linoleate 9/13-lipoxygenase equilibrated in implicit solvent colored according to the RMSD calculated between the backbones of the pairs of corresponding residues from the final conformations in the electric field and control simulations. The regions presenting the largest conformational changes during the dynamics in the presence of the electric field are comprised between residues 19–37, 56–64, 157–173, 300–307, 497–507 and 636–648. These are N- and C-termini and flexible loops exposed on the protein surface. These results show that a short but highly intense pulse is able to produce significant changes in the protein conformation.

Even if the tendencies of RMSD time series presented in Fig. 1a–b are similar, there is a notable difference between the simulations performed in implicit solvent and in vacuum, the simulations performed in vacuum being characterized by smaller RMSD values. These differences are due to the different force fields used in simulations. The one performed in vacuum uses the latest force field [17] that presents an improved sampling of backbone and side chains dihedral angles, which translates into a more stable protein.

The color scale used is presented in the figure: white was used for the regions presenting the lowest displacements, while black was used to represent the regions with the highest displacements, characterized by RMSD values larger than 3 Å, up

to ~9.6 Å. The direction of the applied electric field is also represented on the figure. The figure was generated using UCSF Chimera [22].

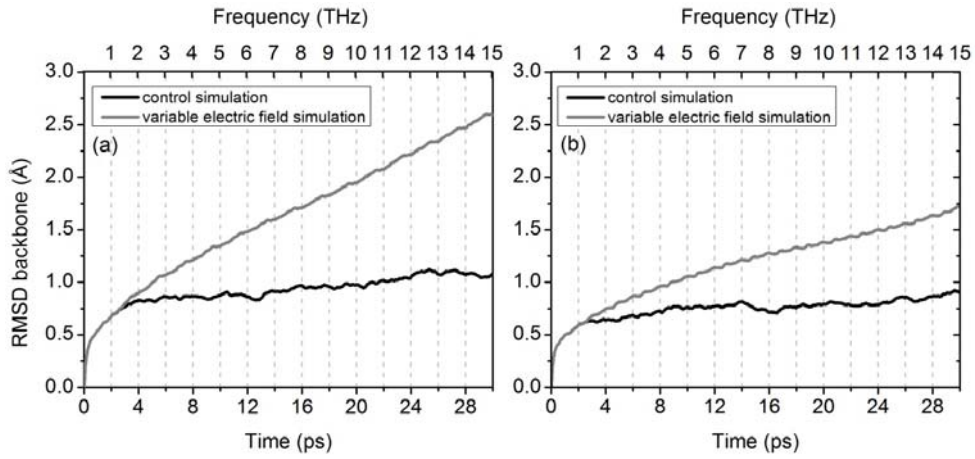

Fig. 1 – RMSD time series calculated for *Pseudomonas aeruginosa* linoleate 9/13-lipoxygenase in control simulation (black line) and in the variable electric field simulations (grey line) relative to the equilibrated structure. The results of the simulations in implicit solvent are plotted in (a) and those obtained in vacuum are plotted in (b). In both plots, the frequencies of the electric field applied in the variable electric field simulations are written on the upper *x* axis.

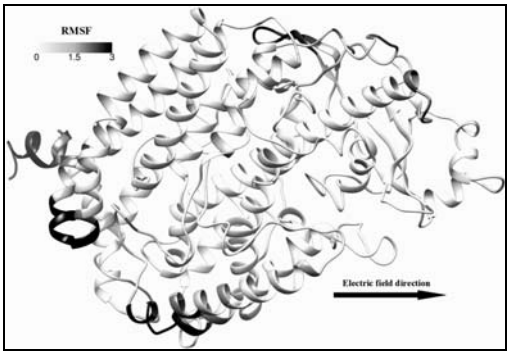

Fig. 2 – The structure of linoleate 9/13-lipoxygenase equilibrated in implicit solvent colored according to the RMSD calculated between the backbones of the pairs of corresponding residues from the final conformations in the electric field and control simulations.

3. EXPERIMENTAL SETUP AND RESULTS

Generation of multiple high-power THz pulses by optical rectification in nonlinear crystals or one color filamentation was reported in ref. [23, 24]. As far as THz electric field is concerned, its value is three fold higher regarding two color

filamentation compared with one color filamentation, due to the combined laser field asymmetry between the fundamental wave and its second harmonic [25].

A new method for multiple high energetic THz pulses generation from two color laser induced plasma filaments was implemented [26]. THz radiation was achieved from plasma filaments arranged in a parallel spatial distribution and being equally time separated. High energy THz pulses with controllable energy ratio and delay were investigated.

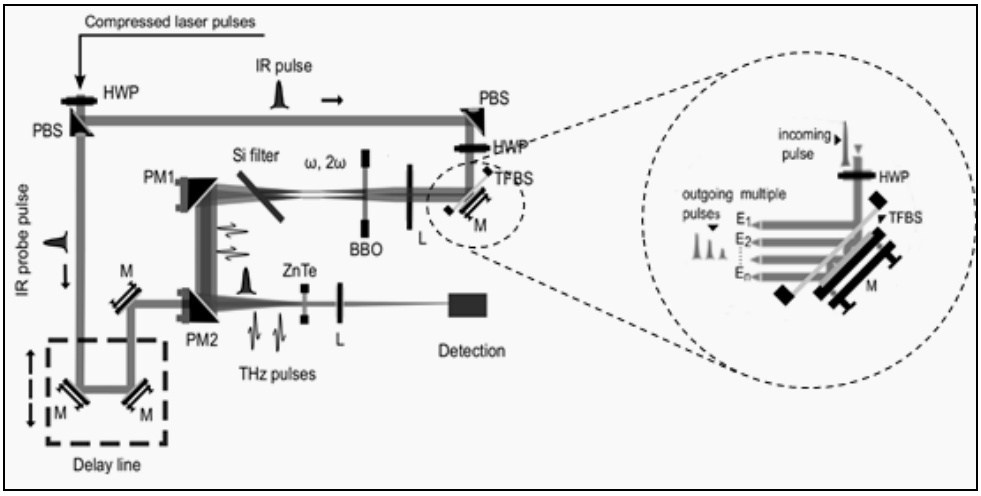

Fig. 3 – Experimental setup for THz emission from multiple filaments. HWP, half-wave plate; PBS, polarizing beam splitter; TFBS, thin film beam splitter; M, 45° high reflectivity dielectric mirrors; L, achromatic lenses; BBO *b*-barium borate crystal, Si filter, silicon filter PM1, PM2, off-axis 90° gold coated parabolic mirrors; ZnTe, zinc telluride crystal; Detection, Z-Omega auto-balanced detector ABL-100.

The experimental setup used to generate and measure high energy THz pulses is depicted in Fig. 3. A Ti:Sapphire laser system at 10 Hz repetition rate and central wavelength at 810 nm delivered 50 fs laser pulses with pulse energy up to 10 mJ. A half-wave plate (HWP) and a polarizing plate beam splitter (PBS) divided the laser beam into two beams. The most intense part was used for two color plasma filament THz generation, while the other part was used as a probe beam for free space electro-optical sampling detection. The first arm of the experimental layout gave rise of air filaments by focusing the laser pulses, fundamental and its second harmonic, with an achromatic lens with 150 mm focal length. Second harmonic generation was obtained by placing a 100 μm thick β-barium borate crystal (BBO) at 60 mm after the lens. The beam had passed through an assembly formed by a thin film beam splitter TFBS polarization sensitive placed between a half-wave plate and a 45° high reflectivity dielectric mirror [27] before it passed

through the lens. This assembly was used in order to obtain several optical sub-pulses from a single laser pulse, as shown in the inset of Fig. 3. A few sub-beams equally time separated following parallel paths are synthesized from de main beam. The delay time could be adjusted by the distance between mirror and TFBS and energy distribution among different optical beams was controlled by the half wave plate orientation.

The energy of each pulse was calculated, taking into the account the laser pulse energy and the reflectance of the TFBS, using the formulae:

$$E_1 = E_T \cdot R, \tag{3}$$

$$E_n = E_T \cdot (1 - R)^2 \cdot R^{n-2},\ n \geq 2, \tag{4}$$

where E_T represents the energy of the fundamental beam before its split and R is the reflectance for a given polarization and tilting. The value of R was adjusted between 10% and 40%.

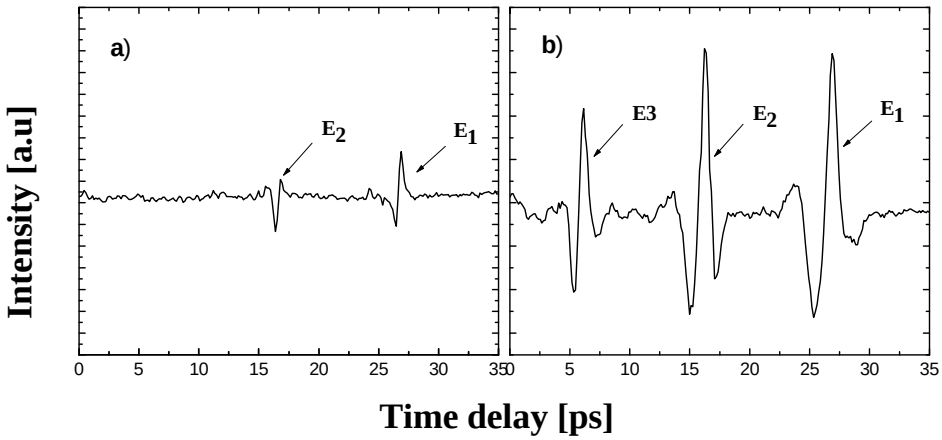

Fig. 4 – Recorded THz waveforms for R coefficient kept at 40% and different amount of total energy E_T: a) 1 mJ, b) 5.3 mJ.

For the highest value of R, the energy of the laser pulses that surpassed the filamentation threshold was found to be equal to 0.4 E_T, 0.36 E_T and 0.14 E_T respectively. Increasing the total energy one increase the number of THz pulses. The recorded THz waveforms for $R = 40\%$ and different amounts of total energy are presented in Fig. 4. THz pulse energy increases with laser pulse energy increasing, having a saturation level above 1.6 mJ laser pulse energy.

For monitoring the time profile of the THz electric field, a 90° off-axis parabolic mirror with 4-inch reflected focal length was used to gather the divergent THz beam emitted by the multiple filaments. A 4 inch pierced off-axis parabolic

mirror combined the THz pulse with the probe beam on a ZnTe crystal in order to measure THz induced birefringence on the electro-optic crystal using an ABL-100 Z-Omega auto-balanced detector.

The total THz energy was measured placing a pyroelectric detector in the focal plane of the second parabolic mirror. For the same laser pulse energy value, one compared the total THz energy emitted by multiple filaments with the THz energy generated by a solitary filament. Above a certain value of pump energy, THz energy obtained using the TFBS method overtook the THz energy produced by a single filament. The time delay between pulses can vary from few to hundreds picoseconds depending on the distance between the mirror and TFBS. The saturation of the THz generation is strongly correlated with the plasma filament condition [28].

4. CONCLUSIONS

Using the TFBS method we succeed to overcome the saturation energy of the THz emission that take place for a single laser pulse induced filament. Intense THz pulses are available at 10Hz repetition rate and consist in trains of two to five pulses with controllable delay from 1 ps to 100 ps and about 2 ps pulse width.

Molecular dynamics simulation results show that the protein undergoes larger conformational changes at the application of very intense variable electric fields than in the control simulation, suggesting that, in practice, intense THz pulses should have at least such an effect. Future work will be focused on a more accurate description of THz pulses in order to reproduce the experimental conditions and to identify which pulses sequence should produce the largest conformational changes and we will also test the reversibility of these changes.

Acknowledgements. Molecular dynamics results are based upon work performed with the computational support of the Computing Centre at the Horia Hulubei National Institute for R&D in Physics and Nuclear Engineering (IFIN-HH), Magurele, Romania. The authors thank PhD. Ionut Vasile for the assistance.

This research was funded by UEFISCDI Romania through the grant PN-II-ID37, grants PCE-2011-3-0801, PCCA-89/2012, PCCA-198/2014 and IDEAS 137/2011 and by EU funding through the project Laserlab Europe 284464.

REFERENCES

1. F. Toschi, F. Lugli, F. Zerbetto, *Effects of electric field stress on a β-amyloid peptide*, J. Phys. Chem. B., **113**, 369–376 (2009).
2. Y.-S. Lee, *Principles of THz Science and Technology*, Springer, 2009.
3. M. Mernea, O. Calorean, O. Grigore, T. Dascalu, D. F. Mihailescu, *Validation of protein structural models using THz spectroscopy: a promising approach to solve three-dimensional structures*, Opt Quant Electron, **46**, 504–514 (2014).

4. A. Garreta, S. P. Val-Moraes, Q. García-Fernández, M. Busquets, C. Juan, A. Oliver, A. Ortiz, B. Gaffney, I. Fita, À. Manresa, X. Carpena, *Structure and interaction with phospholipids of a prokaryotic lipoxygenase from Pseudomonas aeruginosa*, FASEB J., **27**, *12*, 4811–21 (2013).
5. J. Lee, N. Koo, D. B. Min, *Active Oxygen Species, Aging, and Antioxidative Nutraceuticals*, Comprehensive Reviews in Food Science and Food Safety, **3**, 21–33 (2004).
6. A. Di Venerea, E. Nicolaia, I. Ivanovb, E. Dainesec, S. Adelb, B. C. Angeluccic, H. Kuhnb, M. Maccarroned, G. Mei, *Probing conformational changes in lipoxygenases upon membrane binding: Fine-tuning by the active site inhibitor ETYA*, Biochimica et Biophysica Acta (BBA) –Molecular and Cell Biology of Lipids, **1841**, *1*, 1–10 (2014).
7. M. Massaouti, C. Daskalaki, A. Gorodetsky, A. D. Koulouklidis, S. Tzortzakis, *Detection of Harmful Residues in Honey Using Terahertz*, Applied Spectroscopy, **67**, *11*, 1264–1269 (2013).
8. K. B. Ozanyan, P. Wright, M. R. Stringer, R. E. Miles, *Hard-field THz tomography*, IEEE Sens J, **11**, 2507–2513 (2011).
9. J. Federici, D. Gary, R. Barat, D. Zimdars, *THz standoff detection and imaging of explosives*, Proc. SPIE, **5781**, *75* (2005).
10. S. J. Oh, S. H. Kim, K. Jeong, Y. Park, Y.-M. Huh, J.-H. Son, J.-S. Suh, *Measurement depth enhancement in terahertz imaging of biological tissues*, Optics Express, **21**, *18* (2013).
11. L. V. Titova, A. K. Ayesheshim, A. Golubov, D. Fogen, R. Rodriguez-Juarez, F. A. Hegmann, O. Kovalchuk, *Intense THz pulses cause H2AX phosphorylation and activate DNA damage response in human skin tissue*, Biomedical Optics Express, **4**, *4*, 559–568 (2013).
12. W. Berry, C. Jarrahi, *Terahertz generation using plasmonic photoconductive gratings*, New Journal of Physics, **21**, *14*, 17221–7 (2012).
13. J. A. Fulop, Z. Ollmanu, C. Lombosi, C. Scrobol, S. Klingebiel, F. Palfalvi, F. Krausz, S. Karsch, J. Hebling, *Efficient generation of THz pulses with 0.4 mJ energy*, Optics Express, **22**, *17* (2014).
14. C. Vicario, M. Jazbinsek, A. V. Ovchinniko, O. V. Chefonov, S. I. Ashitkov, M. B. Agranat, C. P. Hauri, *High efficiency THz generation in DSTMS, DAST and OH1 pumped by Cr:forsterite laser*, Optics Express, **23**, *4* (2014).
15. N. V. Vvedenskii, A. I. Korytin, V. A. Kostin, A. A. Murzanev, A. A. Silaev, A. N. Stepanov, *Two-Color Laser-Plasma Generation of Terahertz Radiation Using a Frequency-Tunable Half Harmonic of a Femtosecond Pulse*, Physical Review Letters, **112** (2014).
16. B. R. Brooks, Robert E. Bruccoleri, B. D. Olafson, David D. States, S. Swaminathan, M. Karplus, *CHARMM: A Program for Macromolecular Energy, Minimization, and Dynamics Calculations*, J. Comp. Chem., **4**, 187–217 (1983).
17. R. B. Best, X. Zhu, X., J. Shim, P. E. Lopez, J. Mittal, M. Feig, A.D. MacKerell Jr., *Optimization of the additive CHARMM all-atom protein force field targeting improved sampling of the backbone phi, psi and sidechain chi1 and chi2*, JCT, **8**, 3257–73 (2013).
18. T. Lazaridis, M. Karplus, *Discrimination of the native from misfolded protein models with an energy function including implicit solvation*, J. Mol. Biol., **288**, 477–87 (1999).
19. E. Barth, K. Kuczera, B. Leimkuhler, R. Skeel, *Algorithms for constrained molecular dynamics*, J. Comput. Chem., **16**, *10*, 1192–1209 (1995).
20. V. Maiorov, G. Crippen, *Significance of Root-Mean-Square Deviation in Comparing Three-dimensional Structures of Globular Proteins*, Journal of Molecular Biology, **235**, *2*, 625–34 (1994).
21. W. Humphrey, A. Dalke, K. Schulten, *VMD: visual molecular dynamics*, J. Mol. Graph., **14**, *1*, 33–38, 27–38 (1996).
22. E. Pettersen, T. Goddard, C. Huang, G. Couch, D. Greenblatt, E. Meng, T. Ferrin, *UCSF Chimera – a visualization system for exploratory research and analysis*, J. Comput. Chem., **25**, *13*, 1605–12 (2004).
23. M. Durand, Y. Liu, A. Houard, A. Mysyrowicz, *Fine Control of THz radiation from filamentation by molecular lensing in air*, Optics Letter, **35**, *10*, 1710–1712 (2010).

24. Y. Liu, A. Houard, B. Prade, S. Akturk, A. Mysyrowicz, *Terahertz Radiation Source in Air Based on Bifilamentation of Femtosecond Laser Pulses*, Physical Review Letters, **99**, 135002 (2007).
25. T.-J. Wang, S. Yuan, Y. Chen, S. L. Chin, *Intense broadband THz generation from femtosecond*, Chinese Optics Letters, **11**, *1* (2013).
26. R. G. Ungureanu, O. V. Grigore, M. P. Dinca, G. V. Cojocaru, D. Ursescu, T. Dascalu, *Multiple THz pulse generation with variable energy ratio and delay*, Laser Physics Letters, **045301**, *12*, 1612–8 (2015).
27. G. V. Cojocaru, *Thin film beam splitter multiple short pulse generation for enhanced Ni-like Ag x-ray laser emission*, Optics Letters, **39**, *8*, 2246–249 (2014).
28. T. I. Oh, Y. S. You, N. Jhajj, E. W. Rosenthal, H. M. Milchberg, K. Y. Kim, *Scaling and saturation of high-power terahertz radiation generation in two-color laser filamentation*, Appl. Phys. Lett., **102**, 201113 (2013).